Clinical implementation of deep learning: Automatic contouring via U-Net architecture

Matthew Cooper¹ Simon Biggs² Yu Sun¹

Yu Sun¹ Matthew Sobolewski²

Thesis: github.com/matthewdeancooper/masters_thesis

Video overview: docs.pymedphys.com/background/autocontouring







¹Institute of Medical Physics, The University of Sydney

²Riverina Cancer Care Centre, Cancer Care Associates.

Contouring - Current limitations

Variability

- Large intra and inter-observer variance (IOV).¹
- AAPM TG275 risk assessment multiple human-factor failure modes in RT.²

Time constraints

Atlas methods
 ⇒ significant correction times.³

Deep learning potential

- Shown to reduce IOV and contouring time.³
- Significant improvement cf. atlas methods (time & accuracy).⁴

¹Dale Roach et al. "Multi-observer contouring of male pelvic anatomy: Highly variable agreement across conventional and emerging structures of interest". In: Journal of Medical Imaging and Radiation Oncology 63.2 (2019), pp. 264–271. DOI: 10.1111/1754–9485.12844

²Eric Ford et al. "Strategies for effective physics plan and chart review in radiation therapy: Report of AAPM Task Group 275". In: Medical Physics 47.6 (2020), e236–e272. DOI: https://doi.org/10.1002/mp.14030

³Shalini K Vinod et al. "A review of interventions to reduce inter-observer variability in volume delineation in radiation oncology". In: Journal of Medical Imaging and Radiation Oncology 60.3 (2016), pp. 393–406. DOI: 10.1111/1754-9485.12462

⁴Stanislav Nikolov et al. Deep learning to achieve clinically applicable segmentation of head and neck anatomy for radiotherapy. 2018. arXiv: 1809.04430 [cs.CV]

Research goals

Model 1: QA tool (prostate cancer).

- Compare contours to identify macro contouring errors
- Contoured patient, bladder, rectum volumes.

Model 2: Canine vacuum bag.

- Automate time consuming aspect of canine RT.
- \bullet Previously, manual vacuum bag contouring \approx 30 min.

Goal: Performance similar to human experts.

- Performance metric (sDSC) that takes into account expert IOV.⁴
- Stronger correlation with correction time cf. DSC.⁵

³ Shalini K Vinod et al. "A review of interventions to reduce inter-observer variability in volume delineation in radiation oncology". In: Journal of Medical Imaging and Radiation Oncology 60.3 (2016), pp. 393–406. DOI: 10.1111/1754-9485.12462

⁴Stanislav Nikolov et al. Deep learning to achieve clinically applicable segmentation of head and neck anatomy for radiotherapy. 2018. arXiv: 1809.04430 [cs.CV]

⁵Femke Vaassen et al. "Evaluation of measures for assessing time-saving of automatic organ-at-risk segmentation in radiotherapy". In: Physics and Imaging in Radiation Oncology 13 (2020), 1–6. ISSN: 2405-6316. DOI: 10.1016/j.phro.2019.12.001

Performance - Surface dice similarity coefficient (sDSC)

$$DSC_{1,2} = \frac{2|M_1 \cap M_2|}{|M_1| + |M_2|}$$

$$sDSC_{1,2}^{(\tau)} = \frac{|S_1 \cap B_2^{(\tau)}| + |S_2 \cap B_1^{(\tau)}|}{|S_1| + |S_2|}$$

$$M_1 \qquad S_1 \qquad S_1 \qquad S_2^{(\tau)}$$

$$M_2 \qquad S_3 \qquad S_2^{(\tau)}$$

Figure: DSC is a volumetric overlap score, sDSC is a surface overlap score - the percentage of surface contoured within an organ specific tolerance representative of expert IOV.

⁴Stanislav Nikolov et al. Deep learning to achieve clinically applicable segmentation of head and neck anatomy for radiotherapy. 2018. arXiv: 1809.04430 [cs.CV]

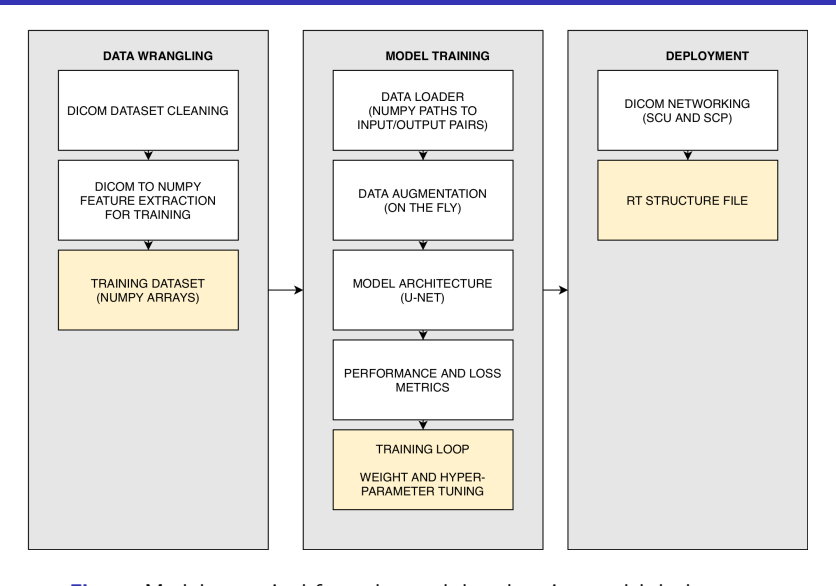


Figure: Modules required for end-to-end deep learning model deployment.

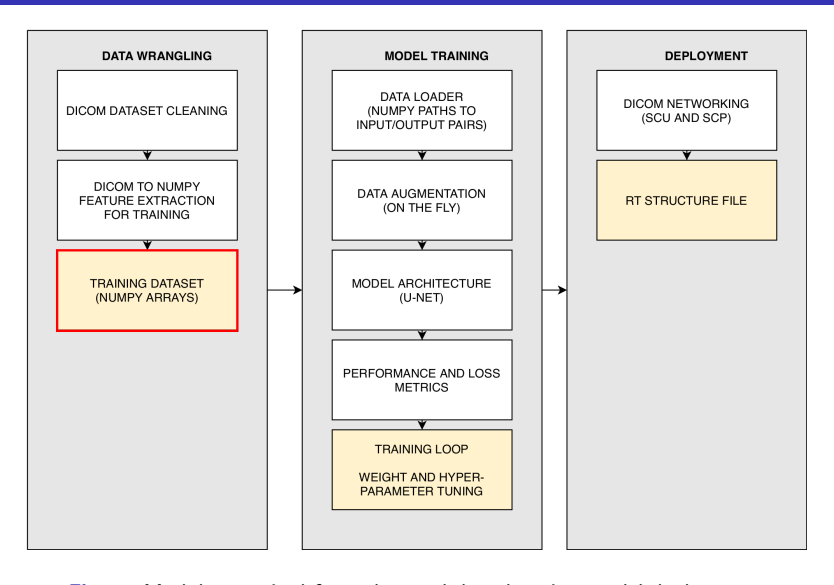


Figure: Modules required for end-to-end deep learning model deployment.

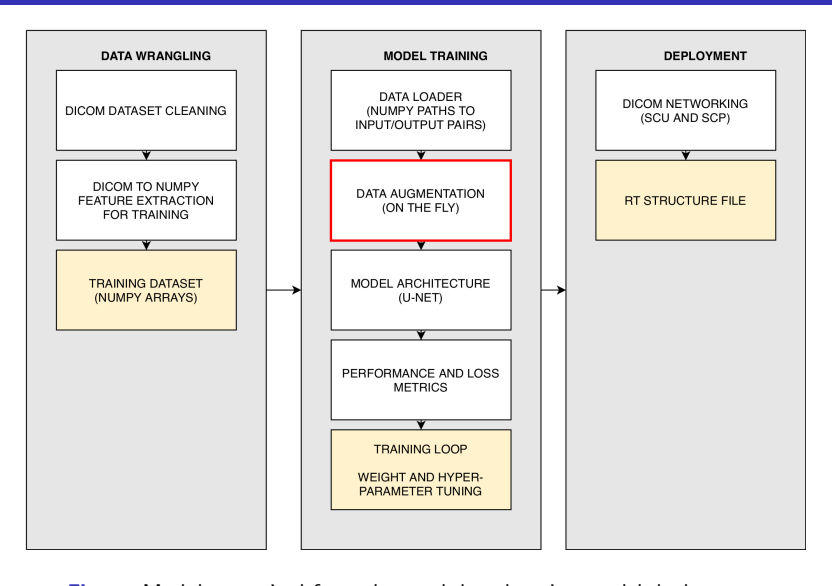


Figure: Modules required for end-to-end deep learning model deployment.

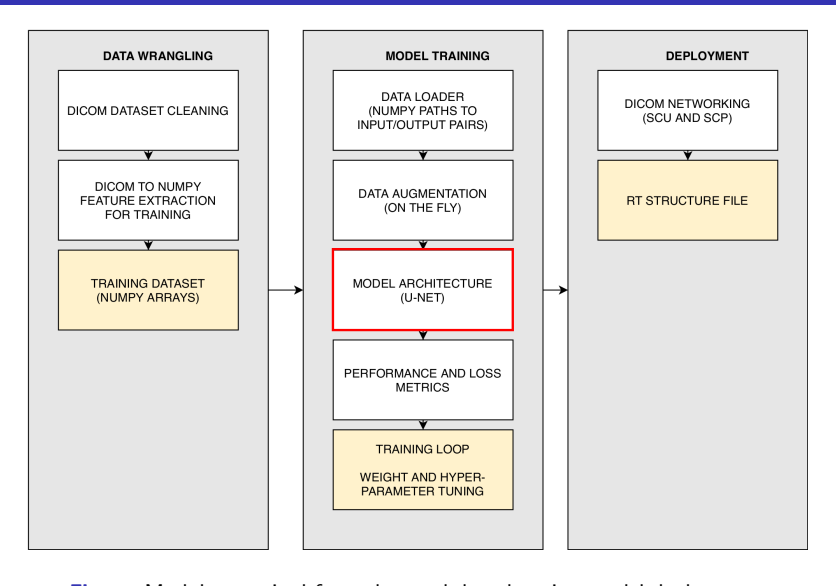


Figure: Modules required for end-to-end deep learning model deployment.

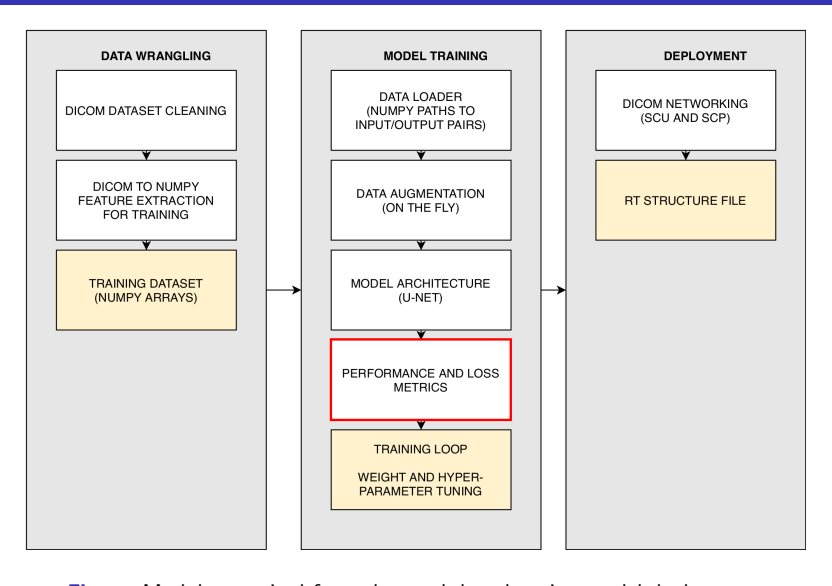


Figure: Modules required for end-to-end deep learning model deployment.

Deployment - DICOM networking

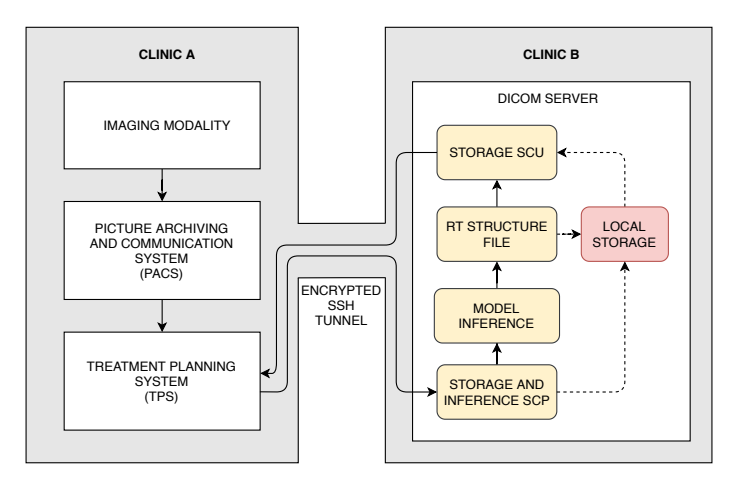


Figure: TPS exports to remote server via DICOM networking protocol.

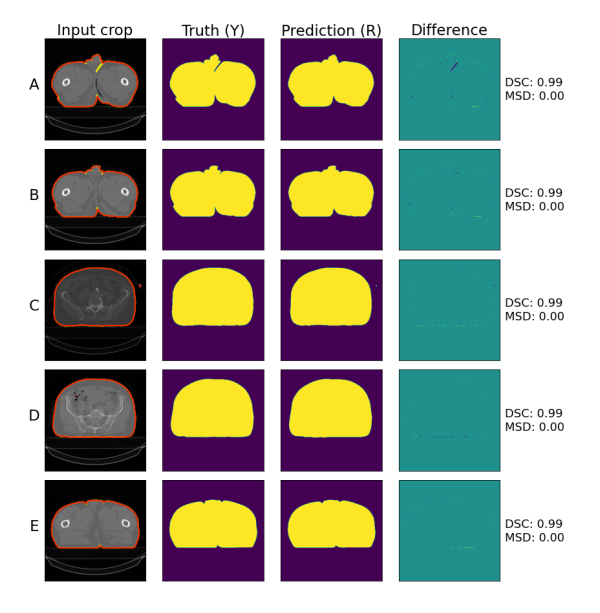


Figure: Representative output for **patient**. Truth contour (yellow), prediction contour (red). Metrics: Dice similarity coefficient (DSC), and mean surface distance (MSD) in mm.

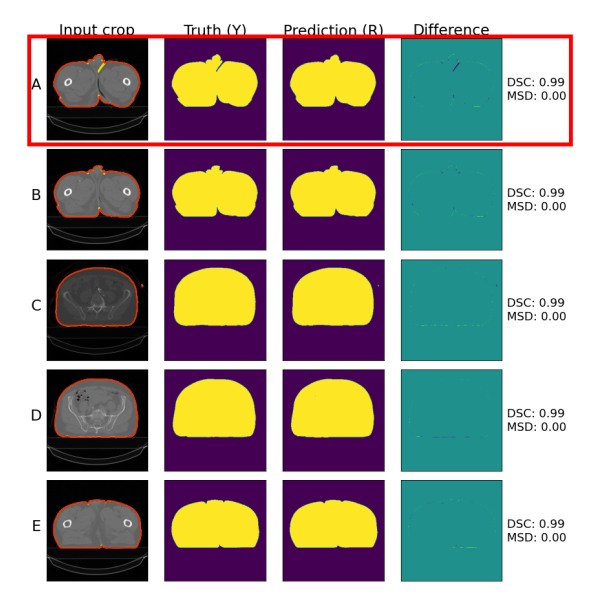


Figure: Representative output for **patient**. Truth contour (yellow), prediction contour (red). Metrics: Dice similarity coefficient (DSC), and mean surface distance (MSD) in mm.

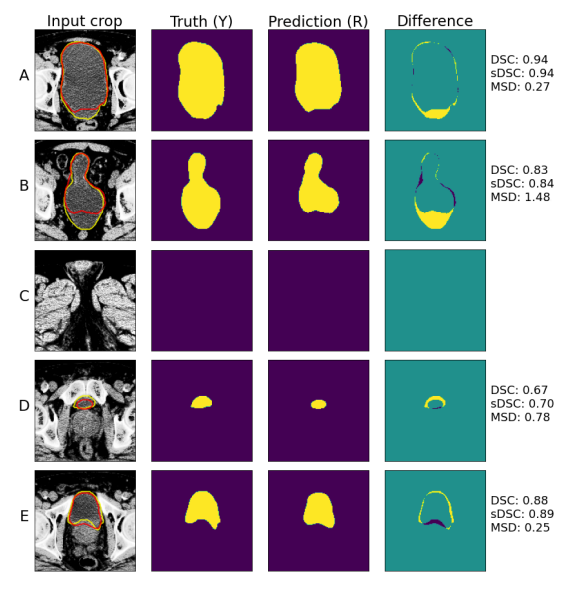


Figure: Representative output for bladder. Truth contour (yellow), prediction contour (red). Metrics: Dice coefficient (DSC), surface dice coefficient (sDSC), and mean surface distance (MSD) in mm.

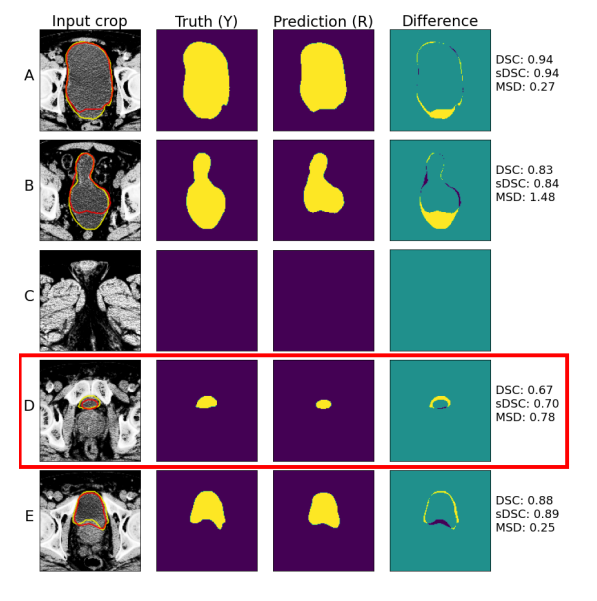


Figure: Representative output for **bladder**. Truth contour (yellow), prediction contour (red). Metrics: Dice coefficient (DSC), surface dice coefficient (sDSC), and mean surface distance (MSD) in mm.

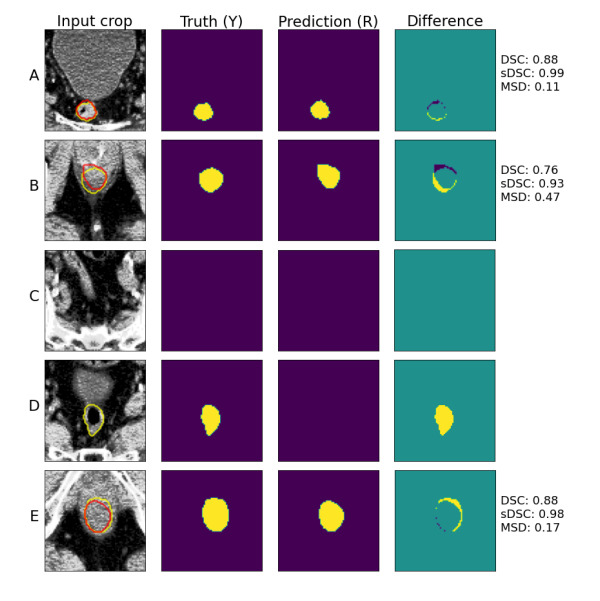


Figure: Representative output for **rectum**. Truth contour (yellow), prediction contour (red). Metrics: Dice coefficient (DSC), surface dice coefficient (sDSC), and mean surface distance (MSD) in mm.

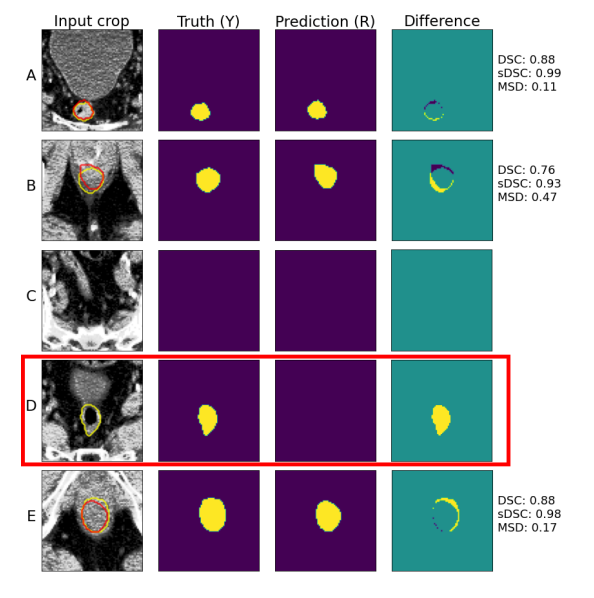


Figure: Representative output for rectum. Truth contour (yellow), prediction contour (red). Metrics: Dice coefficient (DSC), surface dice coefficient (sDSC), and mean surface distance (MSD) in mm.

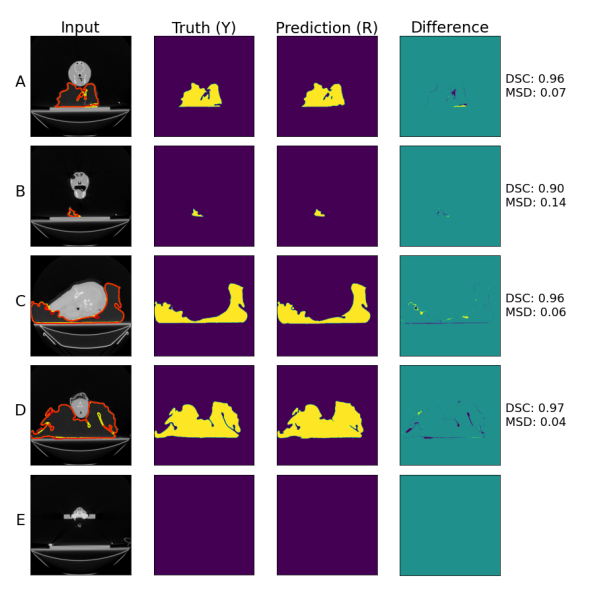


Figure: Representative output for **vacuum bag**. Truth contour (yellow), prediction contour (red). Metrics: Dice similarity coefficient (DSC), and mean surface distance (MSD) in mm.

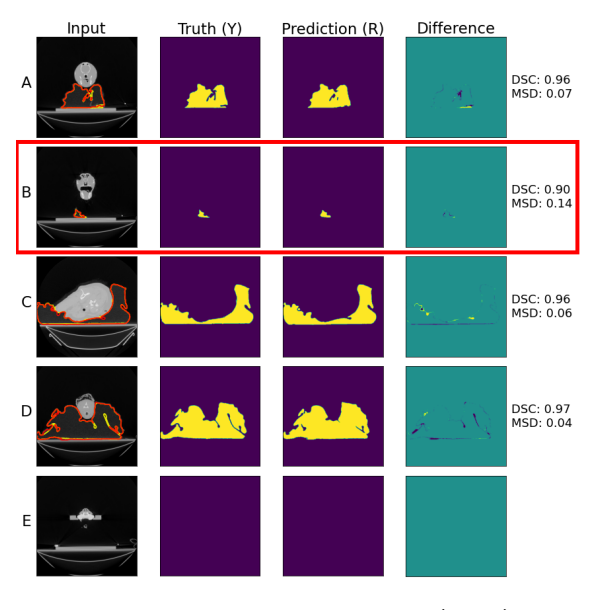


Figure: Representative output for **vacuum bag**. Truth contour (yellow), prediction contour (red). Metrics: Dice similarity coefficient (DSC), and mean surface distance (MSD) in mm.

Structure averaged metrics

Table: Organ specific evaluation on independent dataset.

	sDSC	DSC	MSD (mm)
Pelvic imaging ^a			
Patient		0.99(1)	0.00(5)
Bladder ($ au$ 1.46 mm)	0.9(2)	0.9(2)	1(3)
Rectum (τ 6.99 mm)	0.9(1)	0.7(1)	1(2)
Average	()	0.9(2)	$0.\hat{6}(2)$
Canine imaging			
Vacbag		0.952(1)	0.2(3)
3.0	MCD	/T 0F0/	

 $^{^{\}rm a}$ Organ specific tolerance $\tau={\rm MSD_{95}}$ (Top 95% expert performance).

Cf. expert IOV.1

 \bullet Clinically 'acceptable' bladder and rectum DSC ≥ 0.7

• Bladder: DSC 0.93(3), MSD 0.9(3) mm.

Rectum: DSC 0.81(7), MSD 3(2) mm.

¹Dale Roach et al. "Multi-observer contouring of male pelvic anatomy: Highly variable agreement across conventional and emerging structures of interest". In: Journal of Medical Imaging and Radiation Oncology 63.2 (2019), pp. 264–271. DOI: 10.1111/1754-9485.12844

Conclusion and future work

Pelvic imaging model:

- Patient contouring within tolerances.
- Suspect more data will improve bladder and rectum segmentation.
- 3D architecture may improve detection of gaseous rectal volumes.

Canine imaging model:

- Successfully deployed to clinic under a prototype warning.
- Performance improvement of approximately 30 minutes per patient.

Future

• Develop a continuous valued surrogate for sDSC to optimise directly.



Video overview: docs.pymedphys.com/background/autocontouring

References I

- Ford, Eric et al. "Strategies for effective physics plan and chart review in radiation therapy: Report of AAPM Task Group 275". In: Medical Physics 47.6 (2020), e236–e272. DOI: https://doi.org/10.1002/mp.14030.
- Nikolov, Stanislav et al. Deep learning to achieve clinically applicable segmentation of head and neck anatomy for radiotherapy. 2018. arXiv: 1809.04430 [cs.CV].
- Roach, Dale et al. "Multi-observer contouring of male pelvic anatomy: Highly variable agreement across conventional and emerging structures of interest". In: *Journal of Medical Imaging and Radiation Oncology* 63.2 (2019), pp. 264–271. DOI: 10.1111/1754-9485.12844.
- Vaassen, Femke et al. "Evaluation of measures for assessing time-saving of automatic organ-at-risk segmentation in radiotherapy". In: *Physics and Imaging in Radiation Oncology* 13 (2020), 1–6. ISSN: 2405-6316. DOI: 10.1016/j.phro.2019.12.001.
- Vinod, Shalini K et al. "A review of interventions to reduce inter-observer variability in volume delineation in radiation oncology". In: *Journal of Medical Imaging and Radiation Oncology* 60.3 (2016), pp. 393–406. DOI: 10.1111/1754-9485.12462.